# UV Photosensitivity in a $Ta_2O_5$ Rib Waveguide Mach-Zehnder Interferometer

Chao-Yi Tai, Christos Grivas, and James S. Wilkinson

Optoelectronics Research Center, University of Southampton, Highfield,

Southampton, SO17 1BJ, UK

cyt@orc.soton.ac.uk

Abstract— The UV photosensitivity of $Ta_2O_5$ measured in a rib waveguide Mach-Zehnder interferometer (MZI) is reported. With a cumulative fluence of 72 J/cm$^2$ at a wavelength of 248 nm incident upon one arm through a 3 mm long window, the MZI exhibits a phase shift of $8\pi$ radians at wavelength $\lambda$=1.55 μm, corresponding to a saturated refractive index change of $2.1 \times 10^{-3}$. Real time measurements of the MZI output during exposure are given and the UV-induced refractive index change is found to be negative.

Index Terms— Integrated Optics, Photosensitivity, Mach-Zehnder Interferometer, Planar Lightwave Circuits.

# I. INTRODUCTION

Photosensitive materials have many diverse applications due to the availability of simple, direct and low-cost techniques for optical inscription of microstructures in bulk, thin film and fibre materials. Using photoinduced refractive index change, Bragg gratings are routinely inscribed holographically into the core of fibers [1] and planar waveguides [2]. A variety of guided wave devices including buried channel waveguides [3], directional couplers and power splitters [4] have been demonstrated using the UV direct writing technique.

In response to the rapid growth of DWDM systems and the requirement for low-cost densely integrated optical devices, high refractive index contrast material systems are now being pursued as a platform for the construction of compact planar lightwave circuits. $Ta_2O_5$ is a well-known high refractive index material which may be used on its own, or as a dopant in $SiO_2$ [5]-[6], providing a widely adjustable refractive index by simply varying the $SiO_2/Ta_2O_5$ ratio [7]. While the doped silica systems more readily yield low-loss waveguides, due to lower contrast causing reduced scattering losses, high contrast is required for photonic crystal waveguide applications, rendering pure $Ta_2O_5$ waveguides technologically important. Good quality $Ta_2O_5$ thin films can be reliably produced utilizing several thin film growth techniques [8]-[9], and $Ta_2O_5$ has been widely used as gate material for

microelectronic devices due to its high dielectric constant [9]. However, there are few reports on the great potential of $Ta_2O_5$ for making compact optical waveguide circuits and, in particular, on its photosensitivity [10]. Here, we report the fabrication of a rib waveguide Mach-Zehnder interferometer based on $Ta_2O_5$. A rib waveguide structure with a shallow etch depth was chosen because single mode operation could be achieved with a large modal width, resulting in reduced coupling loss to conventional monomode fibre [11]. Tuning of the MZI phase is achieved by UV light irradiation on one arm of the MZI. The low material absorption throughout the telecommunication wavelength window [12], significant absorption at UV wavelengths, and the potential for high index contrast waveguides makes $Ta_2O_5$ a promising candidate for realizing compact optical waveguide devices.

## II. DEVICE FABRICATION

The top view and the cross-section of the MZI are shown in Figures 1 (a) and 1(b), respectively. In the layout of the MZI, in order to avoid excess radiation loss, the S-bend radius was chosen to be large (63 mm), and the separation between the two arms was chosen to be small (50 μm) to keep the splitting angle of the two S-bends small. The UV exposure window was 3 mm long and sufficiently wide that all the $Ta_2O_5$ in which the mode propagates was irradiated over the 3mm length.

A 1 μm thick layer of $Ta_2O_5$ was first RF sputtered onto a Si wafer with a 2 μm

$SiO_2$ buffer layer, in an $Ar/O_2$ atmosphere with the substrate held at 250°C. During the sputtering process, the chamber pressure was kept at 35 mTorr with $Ar/O_2$ flow rate set to 16 sccm and 6 sccm, respectively. The film was subsequently annealed in pure $O_2$ at 500°C for 12 hours. It is believed that a closely stoichiometric and nearly stress-free film was obtained based on the conditions proposed in [13] [14]. The MZI pattern was formed in a photoresist layer spin-coated onto the $Ta_2O_5$ film, using standard photolithography, and transferred into the $Ta_2O_5$ by argon ion beam milling [15]. The rib waveguides used in the MZI were nominally 2.5 μm wide and were etched to a depth of 150 nm, as shown in Figure 1(b). The shallow etch depth was chosen in order to ensure single mode operation at wavelength $\lambda$=1.55 μm. The MZI waveguides were clad with a 3 μm layer of photoresist (n~1.6), which was overexposed to eliminate the possibility of any further changes in index due to subsequent UV exposure. The cladding material absorbs UV, so that a window is opened in it over one waveguide to allow localized exposure. However, to ensure that no residual UV penetrates the cladding and exposes other parts of the structure, an additional 150 nm thick layer of Au, acting as a light blocking layer, was sputtered onto the device and the 3 mm long window was opened , over one arm of the MZI, in both the gold and the photoresist, to enable UV exposure of that arm alone. This procedure allows a large area of the sample to be illuminated by the excimer laser

beam, while only the desired part of the waveguide circuit is exposed, eliminating the need for precise alignment in the UV-writing setup.

## III. Experiment and Results

Prior to the UV irradiation, the propagation loss of a straight rib waveguide with the same cross-section was measured to be 1.6dB/cm using the cut-back technique, and the waveguide confirmed to be monomode. The absorption spectrum for a 1 μm thick $Ta_2O_5$ thin film sputtered on a $CaF_2$ substrate was measured by spectrophotometry and is shown in Fig. 2. The strong absorption below $\lambda$=263 nm indicates that there is potential for UV irradiation below this wavelength to result in an index change. Ultraviolet light from an excimer laser operating at wavelength $\lambda$=248 nm, with a repetition rate of 1 Hz and a pulse duration of 20 ns, was directed toward to the region to be exposed on the MZI. Prior to exposure of the sample itself, the beam was focused and adjusted through an aperture until the energy was evenly distributed over a spot of diameter 16 mm. This was accomplished by visually inspecting the image recorded on thermally sensitive paper. The energy density for each single shot was measured to be 0.024 J/cm$^2$. A DFB laser operating at $\lambda$=1550 nm, with a polarization maintaining (PM) fibre pigtail, was on-off modulated with a square wave at 1 kHz and the output radiation end-fire launched into the MZI in the TE polarisation. The output of the MZI was directed onto an InGaAs detector through a 40× microscope

objective. The signal was then fed into a lock-in amplifier and was monitored and acquired by a computer.

Figure 3 shows the normalized output power as a function of the exposure time. The periodic modulation characteristic arises from the UV induced phase shift according to:

$$\Delta\phi = \frac{2\pi\Delta N_{eff} L}{\lambda} \quad (1)$$

where $\Delta N_{eff}$ is the effective refractive index change, L is the length of the exposed region (3 mm), and $\lambda$ is the wavelength. The output power response of the MZI is described by:

$$P_{out} = P_{in} \cos^2(\tfrac{1}{2}\Delta\phi) \quad (2)$$

A $\pi$ radian phase shift requires an effective index change of 0.00025 according to (1), for the wavelength and length under consideration. As the differential phase shift increased with fluence, the MZI cycled through several on and off states with an extinction ratio of -13 dB. This extinction ratio is believed to be limited by the contribution of scattered light not passing through the MZI, being collected by the lens. With a cumulative fluence of 72 J/cm$^2$, a total phase shift of $8\pi$ radians was observed, corresponding to a refractive index change of 0.0021. The chirped modulation period shows that the rate of induced index change reduces with exposure energy and saturates with longer exposure time. Figure 3 shows that the calculated

index change decays approximately exponentially with exposure time. The noisy behavior after 1500 seconds is attributed to the degraded stability of the alignment of the apparatus. The long-term stability of the index change is under investigation.

To determine whether the induced refractive index change is positive or negative, a further experiment was performed on a rib waveguide Y junction as shown in Fig. 4(a). The waveguides are the same as those in the MZI, with an identical device being cleaved in half to produce two Y-junctions. A window was opened, in a UV blocking layer, on one arm of a Y-branch and part of the input waveguide, as shown by the enclosed region in Fig. 4(a). UV irradiation was carried out as with the MZI, and the power splitting ratio was monitored. Fig. 4(b) shows the modal power distributions for the post-trimmed Y-junction, and their relative intensity indicates the output power ratio. Before exposure the power splitting ratio was 50:50 with ±1% estimation error, and this was trimmed to 46:54 after ~3000 shots, showing a decreased power output from the branch exposed to UV. This structure with reduced refractive index $\Delta n$=-0.0021 in the enclosed region was simulated by the beam propagation method (BeamPROP™), and the modal power evolution along the Y-junction was plotted in Fig. 4(c). The power splitting ratio at the end of the Y branch was found to be 40:60, in reasonable agreement with the experimental result. The discrepancy between theory and experiment is believed to be due to inaccuracy in placing the UV blocking

mask, which is modeled to be precisely aligned along the centre of the 2.5 μm wide input waveguide. Since there is no noticeable degradation of the modulation visibility in Fig. 3 as fluence increases, UV induced excess loss at the signal wavelength is ruled out. Therefore, this behavior indicates that UV exposure induces a negative index change in the exposed arm, as the optical power flows preferentially into the arm with the higher refractive index.

## IV. Conclusion

In conclusion, we have fabricated a Mach-Zehnder interferometer using rib $Ta_2O_5$ waveguides and adjusted the optical path length in one branch using UV irradiation. Tuning over 4 periods was achieved through the differential photoinduced phase shift between the two arms of the MZI. The device exhibits an extinction ratio of -13 dB and a negative UV-induced refractive index change of $2.1 \times 10^{-3}$. It is notable that a substantial index change is obtained without any pretreatment such as hydrogen loading, presenting behavior comparable to the intrinsically UV-photosensitive germanosilica glass [16]. This result demonstrates the potential of $Ta_2O_5$ for compact optical waveguide devices in the 1.5 μm telecommunications window, with the advantages of combined UV written and relief waveguide structures, and the flexibility to correct fabrication errors through UV trimming.

## REFERENCES


[1] K. O. Hill, Y. Fujii, D. C. Johnson, and B. S. Kawasaki, "Photosensitivity in optical fiber waveguides: Application to reflection filter fabrication," *Appl. Phys. Lett.*, vol. 32, pp. 647-649, 1978.

[2] J. E. Romàn, and K. A. Winick, "Photowritten gratings in ion-exchanged glass waveguides," *Opt. Lett.*, vol. 18, pp.808-810, 1993.

[3] M. Svalgaard, C. V. Poulsen, A. Bjarklev, and O. Poulsen, "Direct UV writing of buried singlemode channel waveguides in Ge-doped silica films," *Electron. Lett.*, vol. 30, pp. 1401-1403, 1994.

[4] M. Svalgaard, "Direct writing of planar waveguide power splitters and directional couplers using a focused ultraviolet laser beam," *Electron. Lett.*, vol. 33, pp. 1694-1695, 1997.

[5] H. Takahashi, S. Suzuki, and I. Nishi, "Wavelength multiplexer based $SiO_2$-$Ta_2O_5$ arrayed-waveguide grating," *J. Lightwave Technol.*, vol. 12, pp. 989-995, 1994.

[6] S. Sekine, K. Shuto, S. Suzuki, "Low-loss, high-Δ, single-mode channel waveguides for high-density integrated optical devices," *Electron. Lett.*, vol. 25, pp. 1573-1574, 1989.

[7] M. Kobayashi and H. Terui, "Refractive index and attenuation characteristics of $SiO_2$-$Ta_2O_5$ optical waveguide film," *Appl. Opt.*, vol. 22, pp. 3121-3127, 1989.

[8] C. Chaneliere, J. L. Autran, R. A. B. Devine, and B. Balland, "Tantalum pentoxide ($Ta_2O_5$) thin films for advanced dielectric applications," *Mat. Sci. Eng.*, vol. 22, pp. 269-322, 1998.

[9] P. C. Joshi and M. W. Cole, "Influence of postdeposition annealing on the enhanced structural and electrical properties of amorphous and crystalline Ta2O5 thin films for dynamic random access memory applications," *J. Appl. Phys.*, vol. 86, pp. 871-880, 1999.

[10] M. P. Roe, M. Hempstead, J. –L. Archambault, P. St. J. Russell, and L. Dong, "Strong photo-induced refractive index changes in RF-sputtered tantalum oxide planar waveguides," *Proc. CLEO Europe'94*, p. 67, 1994.

[11] R. A. Soref, J. Schmidtchen, and K. Petermann, "Large single-mode rib waveguides in GeSi-Si and Si-on-$SiO_2$," *IEEE J. Quant. Electron.*, vol.27, pp. 1971-1974, 1991.

[12] E. Franke, C. L. Trimble, M. J. Devries, J. A. Woollam, M. Schubert, and F. Frost, "Dielectric function of amorphous tantalum oxide from the far infrared to the deep ultraviolet spectral region measured by spectroscopic ellipsometry," *Jounal Appl. Phys.*, vol.88, pp. 5166-5174, 2000.

[13] J. M. Ngaruiya, S. Venkataraj, R. Drese, O. Kappertz, T. P. Leervad Pedersen, and M. Wuttig, "Preparation and characterization of tantalum oxide films

produced by reactive DC magnetron sputtering," *Phys. Stat. Sol.*, vol.198, pp. 99-110, 2003.

[14] C. Christensen, R. de Reus, and S. Bouwstra, "Tantalum oxide thin films as protective coatings for sensors," *J. Micromech. Microeng.*, vol.9, pp. 113-118, 1999.

[15] K. P. Lee, K. B. Jung, R. K. Singh, S. J. Pearton, C. Hobbs, and P. Tobin, "Comparison of plasma chemistries for dry etching of $Ta_2O_5$," *J. Vac. Sci. Technol. A*, vol.18, pp. 1169-1172, 2000.

[16] M. V. Bazylenko, D. Moss, and J. Canning, "Complex photosensitivity observed in germanosilica planar waveguides," *Opt. Lett.*, vol.23, pp. 697-699, 1998.

**Figure Captions**

Fig. 1. Configuration of the rib waveguide Mach-Zehnder interferometer (MZI): (a) Top view of the MZI. The exposed region is enclosed by a dashed line. (b) Cross-section view of the MZI. The thickness and refractive index of individual layers are: Au (150 nm), S1813 (n=1.6, 3μm), $Ta_2O_5$ (n=2, 1μm) and $SiO_2$ (n=1.46, 2μm).

Fig. 2. Absorption spectrum for 1μm thick $Ta_2O_5$.

Fig. 3. Output power as a function of exposure time. The dashed line shows the calculated refractive index change.

Fig. 4(a) Top view of the rib waveguide Y-junction. The exposed region is enclosed by a dashed line. (b) The output power of the two branches. The inset shows the modal intensity profile recorded by the CCD camera. (c) The same structure simulated by beam propagation method.

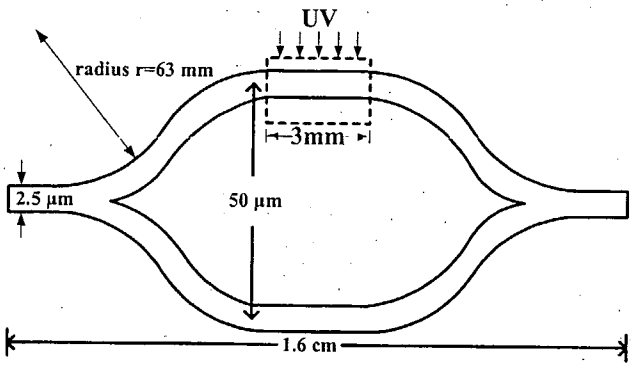
UV
radius r=63 mm
3mm
2.5 µm
50 µm
1.6 cm

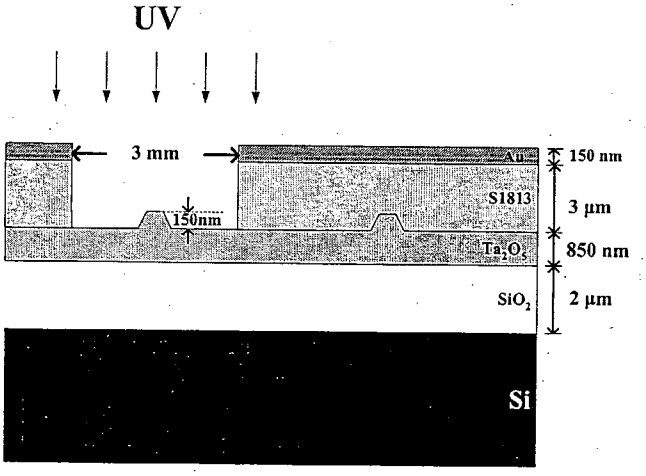
UV
3 mm
150nm
Au
S1813
Ta2O5
SiO2
Si
150 nm
3 µm
850 nm
2 µm

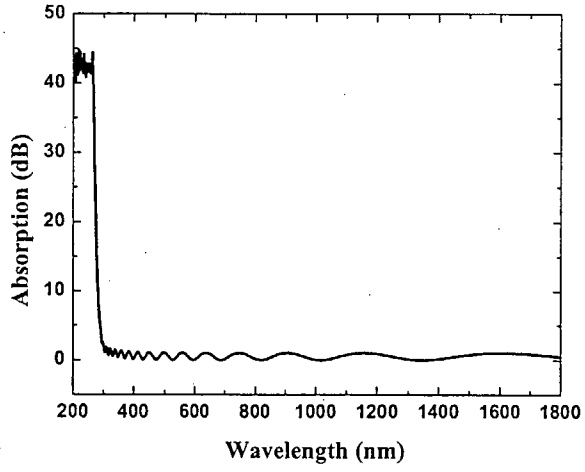
Absorption (dB)
50
40
30
20
10
0
200
400
600
800
1000
1200
1400
1600
1800
Wavelength (nm)

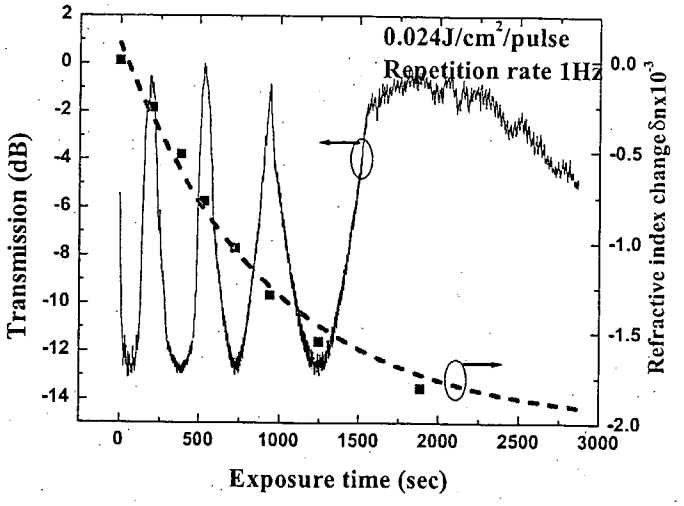
0.024J/cm²/pulse
Repetition rate 1Hz
Transmission (dB)
Refractive index change δnx10⁻³
Exposure time (sec)
2
0
-2
-4
-6
-8
-10
-12
-14
0.0
-0.5
-1.0
-1.5
-2.0
0
500
1000
1500
2000
2500
3000

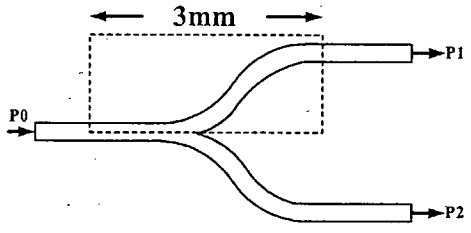
3mm
P0
P1
P2

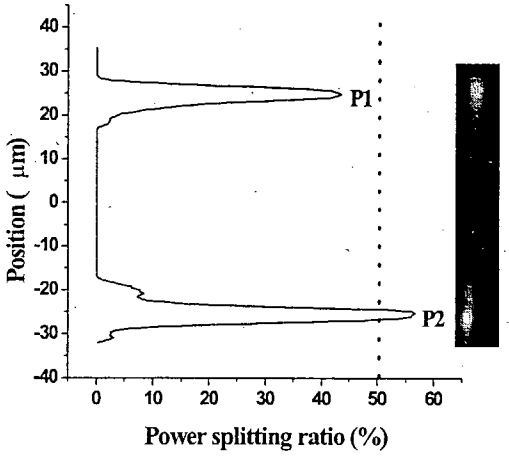
Position ( μm)
40
30
20
10
0
-10
-20
-30
-40
P1
P2
0
10
20
30
40
50
60
Power splitting ratio (%)

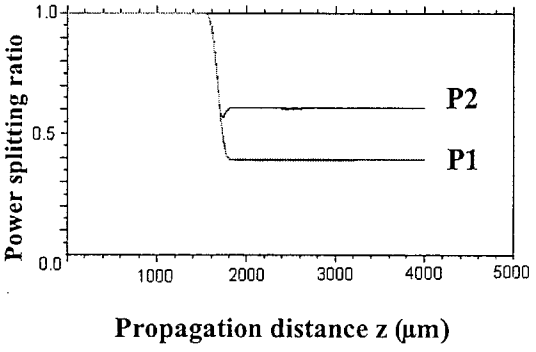
Power splitting ratio
1.0
0.5
0.0
P2
P1
1000
2000
3000
4000
5000
Propagation distance z (μm)